



Enhancing the Light Harvesting Capability of a Photosynthetic Reaction Center by a Tailored Molecular Fluorophore**

Francesco Milano, Rocco Roberto Tangorra, Omar Hassan Omar, Roberta Ragni, Alessandra Operamolla, Angela Agostiano, Gianluca M. Farinola,* and Massimo Trotta*

In memory of Luigi Lopez

Building artificial photosynthetic molecular machines capable of exploiting solar energy for photocatalysis and electrical energy production has attracted considerable interest in recent years.^[1] The studies aim to mimic the main functions of a natural photosynthetic apparatus: harvesting light, converting it into a charge-separated state, and using this state to drive redox reactions such as water splitting.^[2] Photosynthetic organisms share a common functional organization of the protein complexes that form their photosynthetic apparatus. Pigment–protein complexes (the light harvesting complexes) act as antenna, collecting solar light and funneling it to a central photochemical core (the reaction center) where this energy is converted into an electron-hole pair that is eventually used for fueling the metabolism of the organism.^[3]

Ideal biomimetic systems must act as antennas, efficiently harvesting the sunlight and then effectively converting it into a stable charge-separated state with a sufficiently long lifetime to allow ancillary chemistry to take place. The combination of these requirements has not thus far been fully attained: whereas efficient light harvesting and energy transfer have been obtained in artificial systems, the lifetime of charge separated states hardly reaches the millisecond range, thus leading to limited overall energy conversion yields.^[4]

The construction of hybrid systems combining a synthetically tailored antenna with a natural photoconverter appears to be a suitable approach to associate tunable and effective light harvesting with an efficient conversion apparatus that has been optimized by billion years of evolution. Recently, fluorescent quantum dots (QDs) have been proposed as artificial antennas^[5] in a report on the first example of efficient transfer of excitation energy from QDs to a photosynthetic reaction center (RC). In this case, the non-specific electrostatic interactions between the two counterparts prevent the controlled positioning of the artificial antenna with respect to the protein hindering the efficiency of energy transfer processes. Moreover, the size of the bulky spherical-shaped QDs, comparable to the RC one, may represent a drawback for the activity of the hybrid system.

Herein we propose the concept of tailored organic fluorophores as molecular antennas, an approach which offers considerable advantages: the molecular diversity of organic compounds enables very fine tuning of spectroscopic and electronic properties, as well as control of molecular shape and flexibility. This reduces the impact of the artificial antenna on the RC structure and function. Moreover, the chemistry of bioconjugation can affix the fluorophore to selected amino acid residues. We have designed and synthesized a hybrid system combining a bacterial RC with a tailored molecular fluorophore, which acts as an antenna to extend the light harvesting capability of the natural system and enhance its activity in a wavelength range where the unmodified biological system does not efficiently absorb.

The chosen reaction center is the well-known model system isolated from *R. sphaeroides* R26^[7] (Figure 1). It is a membrane-spanning protein composed of three subunits named L, M, and H. Nine cofactors are found in the protein scaffold, two ubiquinone-10 molecules (Q_A, Q_B), one iron ion, two bacteriopheophytins (B Φ), and four bacteriochlorophylls (Bchl), two of which form a functional dimer (D). The purified RC is surrounded by a toroid of detergent molecules,^[8] which prevent its precipitation in water. Upon photon absorption, which occurs with an efficiency close to unity, one electron sitting on D is excited and shuttled to the electron acceptor Q_A and then to Q_B. (Supporting Information, Figure S3.1). In the absence of external reductants, a charge recombination reaction occurs: D⁺Q_B⁻ → DQ_B (or D⁺Q_A⁻ → DQ_A, if the Q_B functionality is inhibited or removed). Conversely, in the presence of an exogenous electron donor to the oxidized D, the RC absorbs a second photon and shuttles a second electron so that the final quinone Q_B, upon

[*] Dr. F. Milano, Prof. A. Agostiano, Dr. M. Trotta
Istituto per i Processi Chimico Fisici
Consiglio Nazionale delle Ricerche
Via Orabona, 4, 70126 Bari (Italy)
E-mail: m.trotta@ba.ipcf.cnr.it

Dr. O. Hassan Omar
Istituto di Chimica dei Composti Organometallici
Consiglio Nazionale delle Ricerche
Via Orabona, 4, 70126 Bari (Italy)

Dr. R. R. Tangorra, Dr. R. Ragni, Dr. A. Operamolla,
Prof. A. Agostiano, Prof. G. M. Farinola
Dipartimento di Chimica
Università degli Studi di Bari Aldo Moro
Via Orabona, 4, 70126 Bari (Italy)
E-mail: farinola@chimica.uniba.it

[**] Ministero dell'Istruzione, dell'Università e della Ricerca (MIUR), and Università degli Studi di Bari Aldo Moro Project PRIN09 PRAM86 "Innovative Materials for Organic and Hybrid Photovoltaics" are acknowledged for their financial support. The COST Action CM0902 "Molecular machineries for ion translocation across biomembranes" is also acknowledged.



Supporting information for this article is available on the WWW under <http://dx.doi.org/10.1002/anie.201203404>.

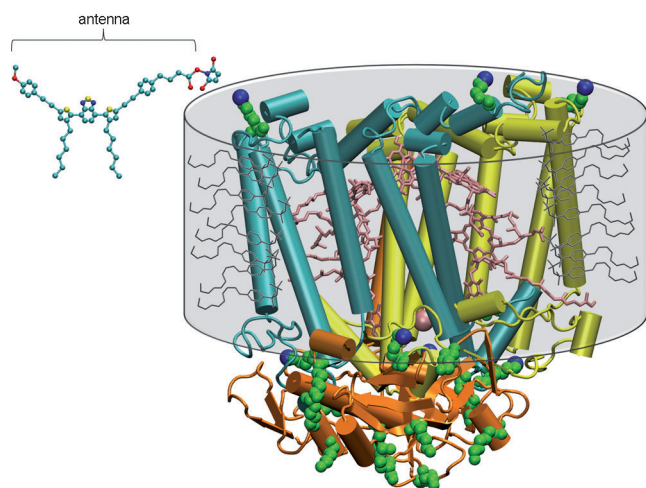


Figure 1. Crystallographic structure of the *R. sphaeroides* R26 reaction center (PDB code: 1AJ1^[6]). Subunits: H orange, L yellow, and M cyan. Bchl, B Φ , and quinones are in pink. The iron ion is a pink van der Waals sphere. Lysines are van der Waals green spheres. The terminal N₂ Lys targets of bioconjugation are in blue. The detergent toroid surrounding the hydrophobic portion of the protein is shown as a grey cylinder, including the detergent molecules (not to scale). The structure of the activated AE antenna is shown in the upper left corner (C cyan, N blue, O red, and S yellow). AE and RC structures are to scale.

double reduction and protonation, is released and substituted by a new quinone molecule from an exogenous pool.^[7] This photocycle can be reconstituted in solution and driven until the exogenous pools of external electron donor (cytochrome) or quinone become exhausted.^[9]

Lysines and cysteines are common targets for the bioconjugation of proteins and enzymes.^[10] In the RC from *R. sphaeroides*, five cysteine residues are present, out of which only H156 is available for bioconjugation.^[11] Conversely, 22 lysines (Lys) are found, nine of which are good candidates for bioconjugation targets because of their positions (see below).

The organic fluorophore AE (Figure 1), which belongs to the class of aryleneethynylenes, has been designed and synthesized^[12] to fulfill the spectroscopic, chemical, and steric requirements to act as antenna for the RC. The conjugated backbone of AE, comprised of a bis(thiophene)-benzothiadiazole core with two phenyleneethynylene arms, absorbs light at 450 nm (where the RC absorption is at a minimum) and has a large Stokes shift with an emission maximum at 602 nm, which corresponds to an RC absorption peak (Figure 2). The succinimidyl ester group in AE enables selective covalent binding of the fluorophore to the Lys of the RC (see the Supporting Information, Section S2). The surfactant Triton X-100 conveys the apolar AE molecules in the aqueous reaction medium, driving them to react with the nine Lys located in proximity to the RC portion surrounded by the Triton X-100 toroid and close to the chlorin pigments (D and Bchl) involved in energy photoconversion. The bioconjugation in this portion of the RC is favored by the intercalation of the n-hexyl chains attached to the thiophene rings of AE with the surfactant molecules surrounding the protein. Moreover, the almost linear shape of AE given by the

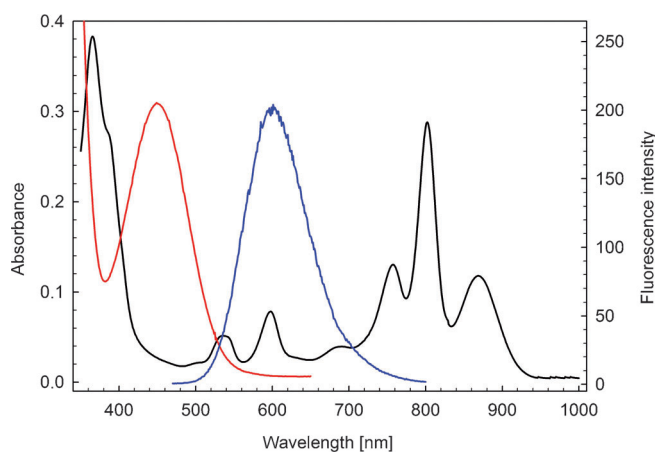


Figure 2. Absorption spectra of RC (—) and AE (—). Fluorescence spectrum of AE (—). RC (1 μ M), AE (4 μ M) in Tris (20 mM), EDTA (1 mM), TX-100 (0.03 %, pH 8; TTE buffer). AE spectra are multiplied by a factor of two. The spectrum of the RC shows several peaks, which arise from the D (860 nm), the monomer Bchl (801 nm), and from the B Φ (765 nm).

presence of the triple bonds, as well as the propyl arm that distances the fluorophore skeleton from its activated carboxyl site are believed to alleviate the steric hindrance of AE molecules on the surface of the RC. All of these features make the reaction highly selective for the functionalization of the protein in the most appropriate positions, thus enabling the RC to be photoactive even at wavelengths where negligible light conversion would normally take place.

The absorption spectrum of the purified AE–RC complex (Figure 3A) confirms bioconjugation, with an average of 4.1 ± 0.3 fluorophores per protein, as calculated from the absorption at 450 nm. Sodium dodecyl sulfate polyacrylamide gel electrophoresis (SDS-PAGE) shows that the binding of AE occurs on all three protein subunits (Figure 3B), showing that Lys are indeed distributed throughout the entire protein (Table S7.1). MALDI-TOF mass measurements show the presence of up to two AEs on the H subunit and up to one on the L and M subunits (Figure S5.1).

The actual AE ability to transfer energy to the RC without significantly modifying the energetics and the activity of the protein was investigated with three different experiments. As a first experiment, the possible alteration of electrochemical midpoint potentials of the semiquinones in the protein (Figure S3.1) were ruled out, as the charge recombination reaction kinetic measured in RC and AE–RC was found to be substantially unchanged. (Figure S4.1).

To verify that bioconjugation to the lysines L82, L268, and M110 close to the binding site of the cytochrome had not jeopardized the correct protein functioning, RC activity was studied by measuring the rate of photocycle in the presence of exogenous cytochrome and quinone. The rate of the photocycle can be obtained by measuring the changes in the absorption intensity at 551 nm, where the difference in absorption between reduced and oxidized cytochrome is at a maximum.^[13] The measurements (Figure 4) were carried out at the diagnostic wavelengths of 600 and 450 nm using a photon flux of $1.50 \times 10^{-2} \mu\text{E s}^{-1} \text{cm}^{-2}$ (corresponding to an

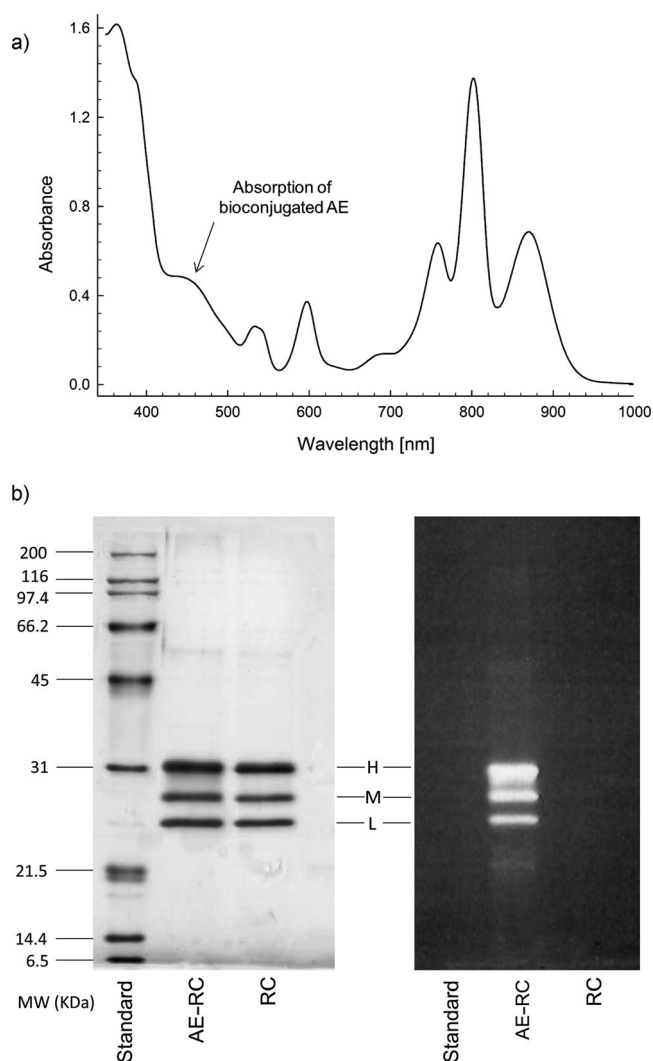


Figure 3. a) Absorption spectrum of the AE-RC molecule. Conditions: RC 4.5 μM in TTE buffer. b) SDS-PAGE of AE-RC and RC. On the left side, the three subunits are clearly visible in both cases (AgNO_3 staining). On the right side, the fluorescence of the bioconjugated subunits is visible under UV light ($\lambda_{\text{ex}} = 302 \text{ nm}$).

irradiance of 3 mW cm^{-2} at 600 nm) in both cases. When illuminated at 600 nm, both RC and AE-RC showed the same rate constant ($3.88 \pm 0.03 \text{ s}^{-1}$ and $3.77 \pm 0.08 \text{ s}^{-1}$ respectively), as the absorption of the protein alone drives the photocycle. At 450 nm, the photocycle was found to be almost three times faster in the AE-RC than in the unmodified protein ($0.78 \pm 0.01 \text{ s}^{-1}$ in RC and $1.90 \pm 0.01 \text{ s}^{-1}$ in AE-RC). This result not only confirms that the bioconjugation is not detrimental to the protein activity but, more importantly, that it enhances the ability of the RC to drive the photocycle.

In a third independent experiment (Figure 5) the antenna effect of the AE was investigated by studying the efficiency of generating the charge separated state in native and functionalized RCs. Under continuous illumination and in the absence of exogenous electron donors, the RC shuttles electrons from the donor to the acceptor and accumulates a charge separated state up to a final concentration that remains constant until the light is switched off. The measurements were again carried

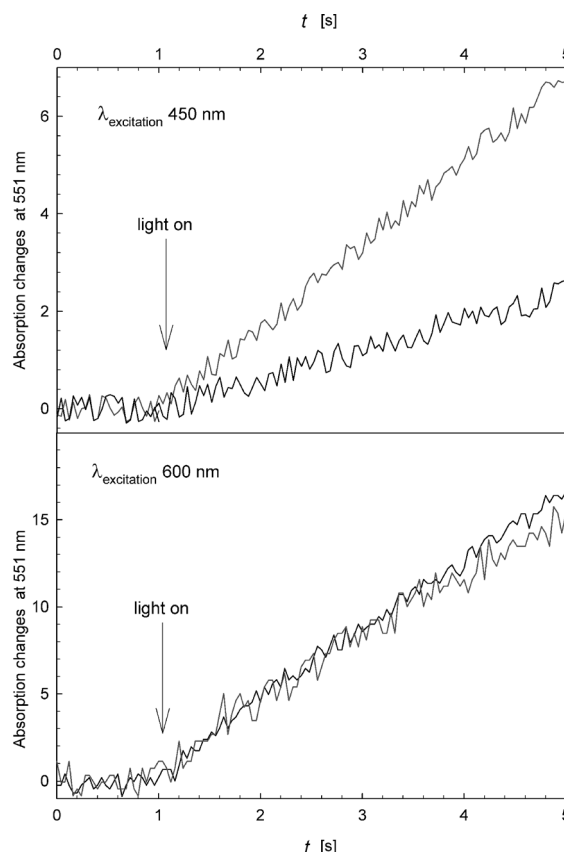


Figure 4. Light driven cytochrome c oxidation at 450 nm (upper) and 600 nm (lower) for RC (—) and AE-RC (---). In both cases, photon flux = $1.50 \times 10^{-2} \mu\text{E s}^{-1} \text{ cm}^{-2}$. Conditions: RC or AE-RC (0.5 μM), Cytochrome c (5 μM), decyl-quinone (50 μM) in TTE buffer with KCl (100 mM).

out at 600 and 450 nm with the same photon flux in both cases. At 600 nm the final concentrations of charge separated RC and AE-RC are coincident. At 450 nm it was observed that the concentration of the charge separated state generated in the AE-RC equals that obtained at 600 nm, whereas in the non bioconjugated protein it is five times smaller.

Time resolved spectroscopy has been used to further characterize the hybrid system. The excited state of AE in buffer solution decays with a single exponential with a lifetime of $6.01 \pm 0.02 \text{ ns}$. The corresponding AE emission spectrum has a maximum at 602 nm. In AE-RC, the fluorescence lifetime is faster, with an average lifetime 2.8 ± 0.1 , and the emission spectrum shows the same maximum position, but with an intensity (after correctign for internal absorption) almost three times smaller than that of AE (Figure 6).

To gain insight into the mechanism for the energy transfer between AE and RC, the Förster distance was calculated for AE ($R_0 = 54 \text{ \AA}$; see the Supporting Information, Section S6). Considering the distance between the nine best candidate lysines and the chlorin pigments (Table S7.3), 26 out of 27 are shorter than the Förster distance, which suggests that energy transfer may occur by fluorescence resonance. Such a fluorescence resonance energy transfer (FRET) mechanism, also proposed in the case of the QDs associated to RC,^[5] would involve any AE molecule bound to any of the nine lysines as

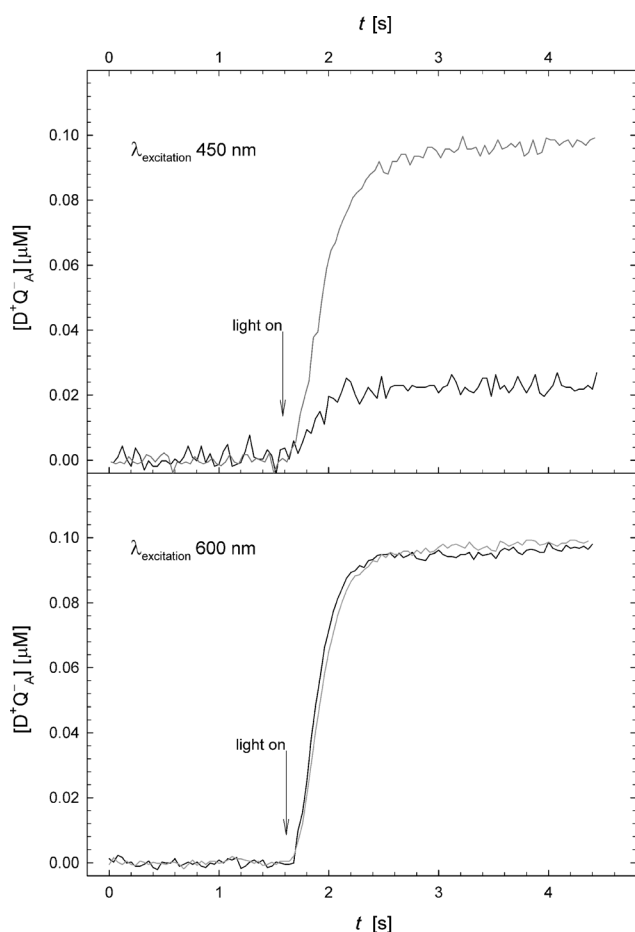


Figure 5. Concentration of $D^+Q_A^-$ generated by continuous illumination at 450 nm (upper) and 600 nm (lower) at photon flux $= 1.50 \times 10^{-2} \mu\text{E s}^{-1} \text{cm}^{-2}$. RC (—) or AE-RC (---) at a concentration of 1 μM in TTE buffer with KCl (100 mM).

donors, transferring energy to any of the chlorin pigments functioning as acceptors.

Altogether the data clearly indicate that the AE covalently binds to the reaction center and correctly functions as an antenna. In fact, at 450 nm the hybrid system outperforms the protein by a factor of three according to the photocycle assay, and by a factor of five according to charge separation and steady state fluorescence measurements. Thus, light collected by the fluorophore at 450 nm is efficiently transferred by a FRET mechanism to the protein, and used for its enzymatic activity without any loss of functional integrity.

In conclusion, we have shown that a tailored molecular organic dye can be covalently conjugated with the photosynthetic RC of *Rhodobacter sphaeroides* to synthesize a hybrid system capable of absorbing light and efficiently performing photoconversion in a wavelength range where the non-conjugated protein does not absorb. This method can selectively functionalize the lysine residues that are best located for efficient energy transfer, and the molecular structure of the AE dye allows the enzyme to maintain full activity. These findings show that it is possible to design effective organic/biological hybrid photosynthetic machines for energy conversion, and paves the way to a new generation

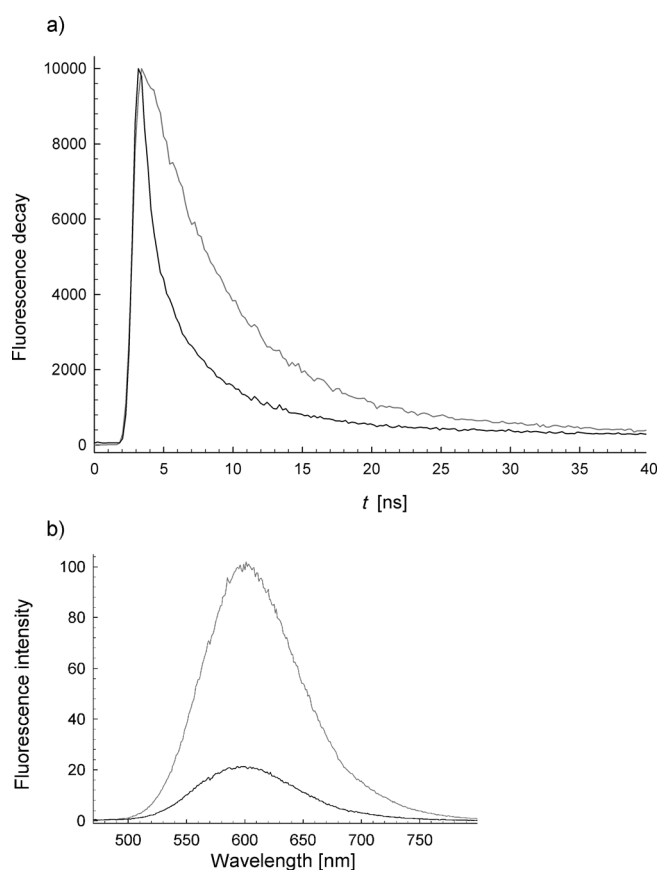


Figure 6. Fluorescence measurements. a) Fluorescence decay of AE (—) and AE-RC (---). b) Steady state fluorescence of AE (—) and AE-RC (---). Excitation wavelength 450 nm. Conditions: AE (4 μM) in the steady state experiment, AE (10 μM) in time resolved experiment. AE-RC (AE/RC = 4:1) in TTE buffer.

of hybrid materials with functional properties going beyond those of natural photosynthetic systems.

Received: May 3, 2012

Published online: September 26, 2012

Keywords: bioconjugation · fluorophores · hybrid structures · photosynthesis · protein modifications

- [1] a) J. Barber, *Chem. Soc. Rev.* **2009**, 38, 185–196; b) P. Maróti, M. Trotta in *CRC Handbook of Organic Photochemistry and Photobiology, Vol. 1*, 3rd ed. (Eds.: A. Griesbeck, M. Oelgemöller, F. Ghetti), CRC, Boca Raton, FL, **2012**.
- [2] A. Sartorel, M. Carraro, F. M. Toma, M. Prato, M. Bonchio, *Energy Environ. Sci.* **2012**, 5, 5592–5603.
- [3] G. D. Scholes, G. R. Fleming, A. Olaya-Castro, R. van Grondelle, *Nat. Chem.* **2011**, 3, 763–774.
- [4] a) V. Balzani, G. Bergamini, P. Ceroni, *Nanopart. Nanodevices Biol. Appl.* **2009**, 4, 131–158; b) V. Balzani, A. Credi, M. Venturi, *ChemSusChem* **2008**, 1, 26–58.
- [5] I. Nabiev, A. Rakovich, A. Sukhanova, E. Lukashev, V. Zagidullin, V. Pachenko, Y. P. Rakovich, J. F. Donegan, A. B. Rubin, A. O. Govorov, *Angew. Chem.* **2010**, 122, 7375–7379; *Angew. Chem. Int. Ed.* **2010**, 49, 7217–7221.

- [6] M. H. Stowell, T. M. McPhillips, D. C. Rees, S. M. Soltis, E. C. Abresch, G. Feher, *Science* **1997**, *276*, 812–816.
- [7] G. Feher, J. P. Allen, M. Y. Okamura, D. C. Rees, *Nature* **1989**, *339*, 111–116.
- [8] M. Roth, A. Lewit-Bentley, H. Michel, J. Deisenhofer, R. Huber, D. Oesterhelt, *Nature* **1989**, *340*, 659–662.
- [9] F. Milano, L. Gerencser, A. Agostiano, L. Nagy, M. Trotta, P. Maróti, *J. Phys. Chem. B* **2007**, *111*, 4261–4270.
- [10] a) G. T. Hermanson, *Bioconjugate Techniques*, 2nd Edition ed., Academic Press, London, UK, **2008**; b) P. Thordarson, B. Le Droumaguet, K. Velonia, *Appl. Microbiol. Biotechnol.* **2006**, *73*, 243–254.
- [11] S. Osváth, J. W. Larson, C. A. Wraight, *Biochim. Biophys. Acta Bioenerg.* **2001**, *1505*, 238–247.
- [12] a) G. M. Farinola, F. Babudri, A. Cardone, O. Hassan Omar, F. Naso, *Pure Appl. Chem.* **2008**, *80*, 1735–1746; b) A. Operamolla, R. Ragni, O. Hassan Omar, G. Iacobellis, A. Cardone, F. Babudri, G. M. Farinola, *Curr. Org. Synth.* **2012**, in press.
- [13] L. Gerencsér, G. Laczkó, P. Maróti, *Biochemistry* **1999**, *38*, 16866–16875.
-